Stat

WILEY

ORIGINAL ARTICLE OPEN ACCESS

A Joint Temporal Model for Hospitalizations and ICU Admissions Due to COVID-19 in Quebec

Mariana Carmona-Baez[1] | Alexandra M. Schmidt[2] | Shirin Golchi[2] | David Buckeridge[2]

[1]Quantitative Life Sciences, McGill University, Quebec, Canada | [2]Department of Epidemiology, Biostatistics, and Occupational Health, McGill University, Quebec, Canada

Correspondence: Mariana Carmona-Baez (mariana.carmonabaez@mail.mcgill.ca)

Received: 2 May 2024 | **Revised:** 8 July 2024 | **Accepted:** 1 August 2024

Keywords: Bayesian inference | count data | disease modelling | dynamic linear model | transfer functions

ABSTRACT

Infectious respiratory diseases have been of interest in recent years for the great burden they place on health systems, for instance, the severe acute respiratory syndrome coronavirus 2 (SARS-CoV-2) that caused the global COVID-19 pandemic. As many of these diseases might require hospitalization and even intensive care unit (ICU) admission, understanding the joint dynamics of hospitalizations and ICU admissions across time and different groups of the population remains of great importance. We aim to understand the joint evolution of hospital and ICU admissions given COVID-19 test-positive cases in the province of Quebec, Canada. We obtain the daily counts, by age group, on the number of confirmed COVID-19 cases, the number of hospitalizations and the number of ICU admissions due to COVID-19, from March 2020 through October 2021 in Quebec. We propose a joint Bayesian generalized dynamic linear model for the number of hospitalizations and ICU admissions to study their temporal trends and possible associations with sex and age group. Additionally, we use transfer functions to investigate if there is a memory effect of the number of cases on hospitalizations across the different age groups. The results suggest that there is a clear distinction in the patterns of hospitalizations and ICU admissions across age groups and that the number of cases has a persistent effect on the rate of hospitalization.

1 | Introduction

Many respiratory diseases might require hospitalization or even ICU admission. A recent example is the severe acute respiratory syndrome coronavirus 2 (SARS-CoV-2) that caused the global COVID-19 pandemic. The first registered case of the disease was located in Wuhan, China, in December 2019, and in March 2020, it was declared a global pandemic (World Health Organization, 2020). Globally, the number of cases summed up to over 630 million as of October 2022. From March 2020 to October 2022, Canada had a total of 4.37 million cases, with Ontario and Quebec being the provinces with the highest incidence.

Some studies suggest that the severity of this disease varies with age and sex. According to Caramelo, Ferreira, and Oliveiros (2020), male patients are more likely to die from COVID-19, and as stated in Davies et al. (2020), age is frequently shown to be a predominant risk factor in the transmission and severity of COVID-19. Aside from the individual's characteristics, vaccination has proven to be effective in preventing acute infections (Lipsitch and Dean 2020). In the United States, vaccination substantially impacted the mitigation of COVID-19 outbreaks and markedly reduced the number of non-ICU hospitalizations, ICU hospitalizations and deaths (Moghadas et al. 2020).

To study the evolution of COVID-19 over time, autoregressive integrated moving average (ARIMA) models and machine learning methods such as artificial neural networks with the main objective of predicting deaths, new cases and outbreaks (Chyon et al. 2022; Jin et al. 2020; Oshinubi et al. 2022) have been used.

When fitting the mentioned models, the time series of different response variables, such as cases and deaths, are usually considered independently.

Our goal is to model the joint distribution of the number of hospitalizations and ICU admissions due to COVID-19 over time in the province of Quebec per age group. We are focused on studying the evolution of daily counts of hospitalizations and the patterns of ICU admissions. To model the number of hospitalizations, we include the proportion of male cases and the proportion of fully vaccinated people as covariates, and to model the number of ICU admissions, we use as covariate the proportion of hospitalized males. By modelling the hospitalizations and ICU admissions simultaneously, we borrow strength across the two-time series. In addition, the proposed hierarchical generalized dynamic linear model (GDLM) allows for information sharing across age groups (West and Harrison 1997). Unlike ARIMA models, GDLMs naturally account for the nonstationarity of the time series and have parameters with clear interpretations.

This paper is organized as follows. The next section describes the data, the proposed model, as well as the inference procedure. Section 3 compares the different fitted models and presents the results from the best model (according to the Watanabe–Akaike information criterion). Section 4 concludes with a discussion.

2 | Methods

2.1 | Data

We consider the daily counts of hospitalizations and ICU admissions by six age groups from 3 March 2020 to 31 October 2021. The data were made available privately by the Institut national d'excellence en sant 'e et en services sociaux (Iness) and consist of 421,416 individuals with a confirmed case, their age, sex, date of admission in case of hospitalization and whether they required ICU admission. A confirmed case is defined as an individual with a positive PCR (polymerase chain reaction) test result for COVID-19. The PCR test for COVID-19 is a molecular test that analyses the upper respiratory specimen, looking for genetic material (ribonucleic acid or RNA) of SARS-CoV-2. The distribution of the observations by age group is shown in Figure 1. We aggregated the data daily and by age group (30–39, 40–49, 50–59, 60–69, 70–79 and 80+). Additionally, we have data on the proportion of fully vaccinated individuals in Quebec from 14 December 2020 to 31 October 2021 (Figure S1). A fully vaccinated individual is defined as someone who received their second dose of the COVID-19 vaccine at least 7 days before the data collection.

From the daily hospitalizations data (Figure S2), we can identify that from the start of March 2020 up until July 2020, Quebec was hit with the first wave of COVID-19. The peak of the hospitalizations occurred in the last 2 weeks of April 2020. The second wave began in August 2020 and lasted until the start of March 2021. By the end of March 2021, a third wave started, and it declined in July 2021. Finally, the last observed wave started in mid-July 2021 that was considerably smaller than the previous ones and more evident for age groups below 50. Age groups 30–39 and 40–49 present the lowest number of hospitalizations, with daily averages of 2.07 and 2.81, respectively. Hospitalizations for age groups 50–59 and 60–69, are two times greater than the previous age groups, in this case, with daily averages of 4.72 and 5.89, respectively. Age group 70–79 has a daily average of 7.42 that is almost four times greater than that of the youngest age group. Finally, the oldest age group (80+) presents the highest number of hospitalizations with a daily average of 12.2, six times greater than the youngest age group. The maximum number of hospitalizations per day corresponds to the 80+ age group with a record of 64 for the observed period.

The pattern of the time series of ICU admissions follows that of observed COVID-19 hospitalizations (Figure S3). For individuals under 40, the waves are less perceptible given that the maximum number of admissions for this age group is 4. For the 80+ age group, the ICU admissions are below the average number of individuals of age groups 60–69 and 70–79. The daily average is 1.08, compared with 1.86 and 1.92, respectively. This pattern is also observed in other studies (Cohen et al. 2021).

2.2 | Proposed Models

2.2.1 | Hospitalizations Model

Let $H_{t,g}$ be the total number of hospitalizations due to COVID-19 in Quebec, at day t and age group g, for $t = 1, \dots, N$, where $N = 608$ is the number of days in the observed period and $g = 1, \dots, G$, where $G = 6$ is the number of age groups considered in the model. We propose a Poisson model for $H_{t,g}$ defined by

$$p\left(H_{t,g}|\lambda^H_{t,g}, e_g\right) \sim \text{Poisson}\left(H_{t,g}|\lambda^H_{t,g}, e_g\right), \tag{1}$$

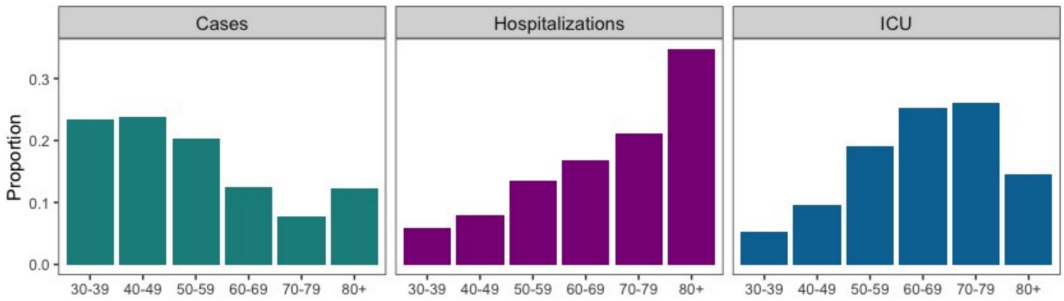

FIGURE 1 | Distribution by age group of COVID-19 cases (green), hospitalizations due to COVID-19 (violet) and ICU admissions due to COVID-19 (blue) from March 2020 to October 2021.

where e_g is an offset and $\lambda^H_{t,g}$ is the rate parameter. Here, the offset is defined such that e_g represents the expected number of cases per 10,000 people per age group.

To model $\lambda^H_{t,g}$, we specified the following log-linear relationship:

$$\log\left(\lambda^H_{t,g}\right) = \alpha^H_{t,g} + \beta^H_g X^{(1)}_{t,g} + \delta X^{(2)}_t + u_{t,g}, \tag{2}$$

where $\alpha^H_{t,g}$ represents the intercept that changes with age group and time, $X^{(1)}_{t,g}$ is the standardized proportion of male cases at day t and age group g, and $X^{(2)}_t$ is the proportion of vaccinated people on day t in the *logit* scale to obtain a more symmetric behaviour of the covariate. Then it follows that the effect of the proportion of male cases at an age group level is denoted by β^H_g, and the effect of the proportion of vaccinated people in Quebec is denoted by δ. The use of the offset leads to the exponentiated regression coefficient of a covariate representing the multiplicative expected rate changes for a one-unit increase in the covariate. In this case, the rate is expressed as the number of hospitalizations per e_g confirmed cases.

We expect a delay in the association between the number of COVID-19 cases and hospitalizations related to the time to develop symptoms. It is then reasonable to assume that the number of cases does not have only an immediate impact on the hospitalizations, but that its effects might propagate in time. Therefore, we propose to model this association through a transfer function model (Alves, Gamerman, and Ferreira 2010). Transfer functions use a structural variable that measures the combined effect of current and past values of the exposure variable on the outcome (Ravines, Schmidt, and Migon 2006). In this case, the exposure variable is the number of COVID-19 cases, and the structural variable is denoted by $u_{t,g}$ and modelled as

$$u_{t,g} = \rho_g u_{t-1,g} + \gamma_g \text{Cases}_{t,g},\ t = 2,\ \ldots N, \tag{3}$$

where ρ_g is the decay factor and γ_g is the instantaneous gain factor. For time, $t = 1$, we assume $u_{1,g} = \gamma_g \text{Cases}_{1,g}$. To understand the lingering effect of the cases, $u_{t,g}$, on the rate of hospitalizations, $\lambda^H_{t,g}$ one can compute the impulse response function (Alves, Gamerman, and Ferreira 2010), which provides the instantaneous effect of cases at lag j on the rate of hospitalizations at present and future times. Following Alves, Gamerman, and Ferreira (2010), solving the difference equation in (3) recursively, results in $u_{t,g} = \gamma_g \text{Cases}_{t,g} + \rho_g \gamma_g \text{Cases}_{t-1,g} + \rho^2_g \gamma_g \text{Cases}_{t-2,g} + \ldots$. The weight, $\rho^j_g \gamma_g$ for, $j = 0,1,2,\ \ldots$, is the impulse response function and can be seen as how a one-unit standard deviation increase in the number of cases at lag j affects the log rate $\lambda^H_{t,g}$. The behaviour of the impulse response function depends on the sign of ρ_g and γ_g. It is required that $|\rho_g| < 1$ for the model to be stable. When $-1 < \rho_g < 0$ the impulse response function has a geometric decay with alternating signs. When $0 < \rho_g < 1$ and $\gamma_g < 0$, it follows a geometric growth pattern, and when $\gamma_g > 0$, it results in a geometric decay pattern. For our problem, it is reasonable to assume the gradual decay of the effect of the cases, hence $0 < \rho_g < 1$. Values of ρ_g close to 1 would imply more persistent effects of the number of cases on the rate of hospitalizations.

2.2.2 | ICU Admissions Model Conditional on Hospitalizations

Let $\text{ICU}_{t,g}$ be the number of hospitalized cases admitted to the ICU due to COVID-19 at day t and age group g. The observed number of ICU admissions has an excess of zeros for some of the age groups (Table S1). To capture this excess of zeros, we propose a Poisson hurdle model, that is, we assume that

$$p\left(\text{ICU}_{t,g} | \phi_{t,g}, \lambda^I_{t,g}, e_g\right) = \begin{cases} \phi_{t,g} & \text{if } \text{ICU}_{t,g} = 0, \\ (1-\phi_{t,g}) \dfrac{\text{Poisson}\left(\text{ICU}_{t,g} | \lambda^I_{t,g}, e_g\right)}{1 - \text{Poisson}\left(0 | \lambda^I_{t,g} e_g\right)} & \text{if } \text{ICU}_{t,g} > 0. \end{cases} \tag{4}$$

We propose the following linear relationship in the *logit* scale for $\phi_{t,g}$ for the probability of not having ICU admissions:

$$\text{logit}(\phi_{t,g}) = \eta_g + \chi_g H_{t-1,g}, \tag{5}$$

where η_g is the intercept by age group and $H_{t-1,g}$ is the standardized number of hospitalizations at time $t-1$ for age group g. The inverse-*logit* of η_g can be interpreted as the probability of having no ICU admissions when the hospitalizations in the previous day were equal to the mean hospitalizations in the observed period. Lastly, $\exp(\chi_g)$ represents the expected change in the odds for a one-unit increase in the hospitalizations of the previous day, measured in standard deviations.

For this model, the rate $\lambda^I_{t,g}$ follows a log-linear relationship

$$\log\left(\lambda^I_{t,g}\right) = \alpha^I_{t,g} + \beta^I_g X^{(3)}_{t,g}, \tag{6}$$

where $\alpha^I_{t,g}$ represents the intercept, and $X^{(3)}_{t,g}$ is the standardized proportion of hospitalized male patients at time t for age group g, and β^I_g represents the effect of this variable on the log of the rate of ICU admissions.

Four different model variations are considered. These models are based on the general structure proposed and consider different specifications for the hurdle probabilities and the transfer function. Model M0 is the simplest version, it does not consider a transfer function and assumes the probabilities of zeros coming from the hurdle component are fixed across time and age groups. Model M1 is similar to model M0 but allows the probabilities associated with the hurdle component to change across time (Equation 5). Model M2 adds the transfer function for the total cases to M0. Lastly, model M3 considers both the transfer function and the time-varying probabilities for the hurdle model.

2.2.3 | Hierarchical Prior Specification

As inference procedure follows the Bayesian paradigm, the model specification requires assigning prior distributions to all the parameters in the model. The intercept in the model for hospitalizations, $\alpha^H_{t,g}$ follows a normal prior distribution with a common mean across all the age groups and an age group-specific standard deviation, that is, $\alpha^H_{t,g} \sim N(\mu^H_t, \sigma^2_g)$. We allowed each

age group to have its standard deviation as the magnitude of the hospitalizations varies considerably between them. The intercept in the ICU admissions model $\alpha^I_{t,g}$ follows a normal distribution with a common mean and standard deviation for all age groups, that is, $\alpha^I_{t,g} \sim N(\mu^I_t, \sigma^2_{\alpha I})$. In this case, in our view, it is not necessary to include age group-specific standard deviations, as the magnitude of ICU admissions is similar across age groups.

To allow for correlation between the temporal rates of hospitalizations and ICU admissions, we assume that the overall means, μ^H_t and μ^I_t, follow a bivariate normal distribution whose mean vector evolves smoothly with time,

$$\begin{pmatrix} \mu^H_t \\ \mu^I_t \end{pmatrix} \Big| \begin{pmatrix} \mu^H_{t-1} \\ \mu^I_{t-1} \end{pmatrix} \sim \mathcal{N}_2\left(\begin{pmatrix} \mu^H_{t-1} \\ \mu^I_{t-1} \end{pmatrix}, \begin{pmatrix} \sigma^2_{\mu_H} & \tau\sigma_{\mu_H}\sigma_{\mu_I} \\ \tau\sigma_{\mu_H}\sigma_{\mu_I} & \sigma^2_{\mu_I} \end{pmatrix} \right), \quad (7)$$

where τ denotes the correlation parameter (Equation 7). We assign a uniform distribution with bounds −1 and 1 as prior for τ.

The coefficients β^H_g and β^I_g follow a normal distribution with common means (ν^H and ν^I) and standard deviations (σ_{β_H} and σ_{β_I}) across all age groups. The mean parameters follow standard normal prior distributions, and the standard deviation parameters follow half-Cauchy prior distributions with location 0 and scale 1.

Regarding the transfer function parameters, we assign independent Uniform(0,1) prior distributions for ρ_g. For γ_g, we assume a zero mean normal prior distribution with some reasonably large variance, to let the data drive the inference of the shape of the impulse response function. The prior distributions for η_g and χ_g are standard normal distributions.

2.2.4 | Inference Procedure

Following Bayes' theorem, the posterior distribution of the parameter vector containing all the unknowns of the model is proportional to the likelihood times prior distribution. Following the specifications previously discussed, the resultant posterior distribution does not have a closed form. We resort to Markov chain Monte Carlo methods to obtain samples from the posterior. In particular, we used Hamiltonian Monte Carlo methods through the software `Stan`, implemented in the R package `rstan` (Stan Development Team (2024). 'RStan: the R interface to Stan' package version 2.21.3; https://mc-stan.org/)

We used `R version 4.1.2` (R Foundation for Statistical Computing, Vienna, Austria) for data processing and analysis. The MCMC procedure consisted of 2 chains of 25,000 iterations each, with a warm-up period of 12,500 iterations and a thinning factor of 4. The chains mixed well, as assessed by the trace plots, effective sample sizes and the potential scale reduction statistic, Rhat (Gelman and Rubin 1992).

3 | Results

The four model variations described in 2.2 were fitted to the available data set. Table 1 summarizes the fitted models. They were compared through WAIC (Watanabe–Akaike information criterion) (Watanabe and Opper 2010). In terms of the WAIC, for which smaller values are preferred, model M0 is the least adequate among the fitted ones. This suggests that including the effect of the number of cases and allowing the probability of not having ICU admissions improves model fitting. From Table 1, it is clear that, according to WAIC, model M3 is the best among the fitted ones. Below, we present the results for this model.

3.1 | Transfer Function

Figure 2 exhibits the point-wise posterior summaries of the exponential of the impulse response functions ($\exp(\gamma_g \rho_g^j)$) on the rate of hospitalizations for all age groups at different lags. The patterns of the transfer functions are quite different across the age groups. According to Table S1, for age groups above 50, the number of cases has a persistent effect on the rate of hospitalizations as ρ_g is close to 1. The impulse response for age groups 30–39 and 40–49 quickly flattens after a lag of 4 days. For the 50–59 age group, an immediate one standard deviation unit increase in the number of cases, increases the risk of hospitalization by 0.8%. Moreover, the impulse response has a very slow decay, showing a 0.4% increase in the risk even after 60 days. Age groups over 60 start with an effect of around 1% for the first lag. Interestingly, their impulse response decays faster than that of 50–59 age group.

Panels of Figure 3 show the first-order multivariate random walk that represents the mean baseline rates (μ^H_t and μ^I_t). The mean baseline rate of hospitalization is six times greater than that of ICU admissions. The hospitalization rate decreases after the first wave and through the consecutive waves, while the rate of ICU admissions persists through the multiple waves of the pandemic.

TABLE 1 | List of the fitted joint models for hospitalizations and ICU admissions (see Equations 3 and 5 for details), along with their WAIC values, which served for selecting the best model among the fitted ones.

Model	Transfer function	Hurdle model probability ϕ	WAIC	*pw*
M0	—	ϕ_g	30310.5	6612.6
M1	—	$\phi_{t,g}$	29,903.4	5736.8
M2	$u_{t,g}$	ϕ_g	30,282.9	6514.2
M3	$u_{t,g}$	$\phi_{t,g}$	*29,865.6*	5643.5

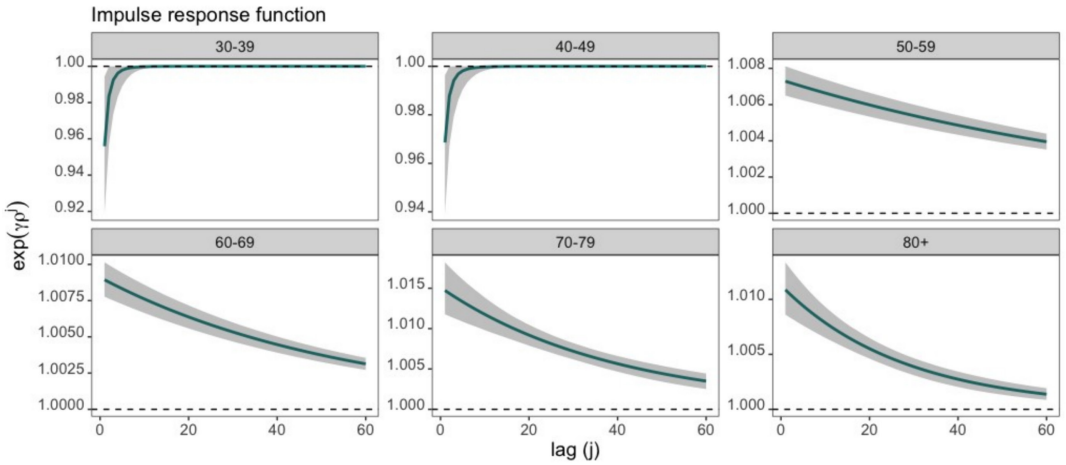

FIGURE 2 | Posterior summaries (mean (solid lines) and limits of 95% posterior credible intervals (shaded area)) of the impulse response functions associated with the total number of cases of COVID-19 by age group.

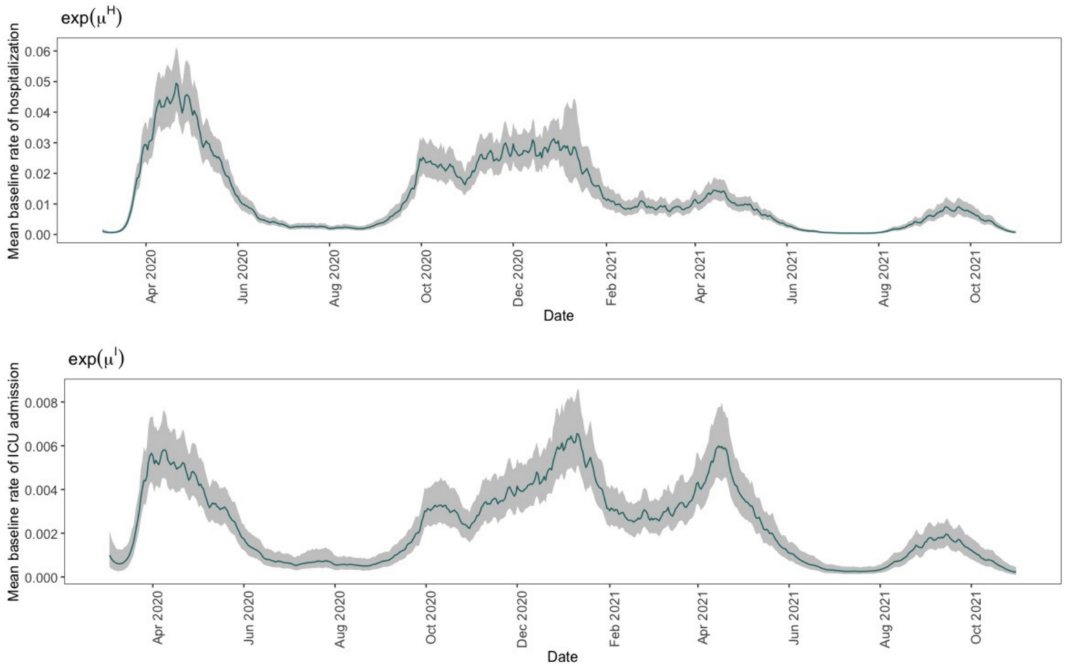

FIGURE 3 | Posterior summaries (mean [solid lines] and limits of 95% posterior credible intervals [shaded area]) of the mean baseline rates of hospitalizations and ICU admissions for each age group. Top panel shows the mean baseline rate of hospitalization, and bottom panel shows the baseline mean of the mean baseline rate of ICU admission.

The posterior mean of the correlation parameter between the mean baseline rates is 0.828 with a 95% credible interval of (0.667, 0.935). Clearly, there is borrow of information in the estimation of the overall (across all age groups), time-varying intercepts of hospitalizations and ICU admissions. This suggests that it is better to model the outcomes jointly than separately.

Figure 4 shows the posterior summaries for the baseline rates of hospitalization (top panel) and ICU admission (bottom panel) per age group $(\exp(\alpha^H_{t,g}), \exp(\alpha^I_{t,g})$, respectively). The COVID-19 waves can be observed in the trajectory of both parameters. At the beginning of the observed period, when the hospitalizations were at their peak, the baseline rate of hospitalization for individuals above 70 is 3 times higher than for individuals below 50. In contrast, the baseline rate of ICU admission has higher peaks for individuals between 50 and 79. This agrees with the data because the youngest and the oldest age groups are the ones with lower incidence of ICU admissions.

Another component in the model is the effect of the proportion of male cases and male hospitalizations. The posterior summaries for these exponentiated coefficients or rate ratio (RR) are shown in Figure 5. For all age groups below 70, the proportion of male cases increases the RR of hospitalizations. For instance, for individuals between 50 and 59 an increase of one standard deviation in the proportion of male cases increases

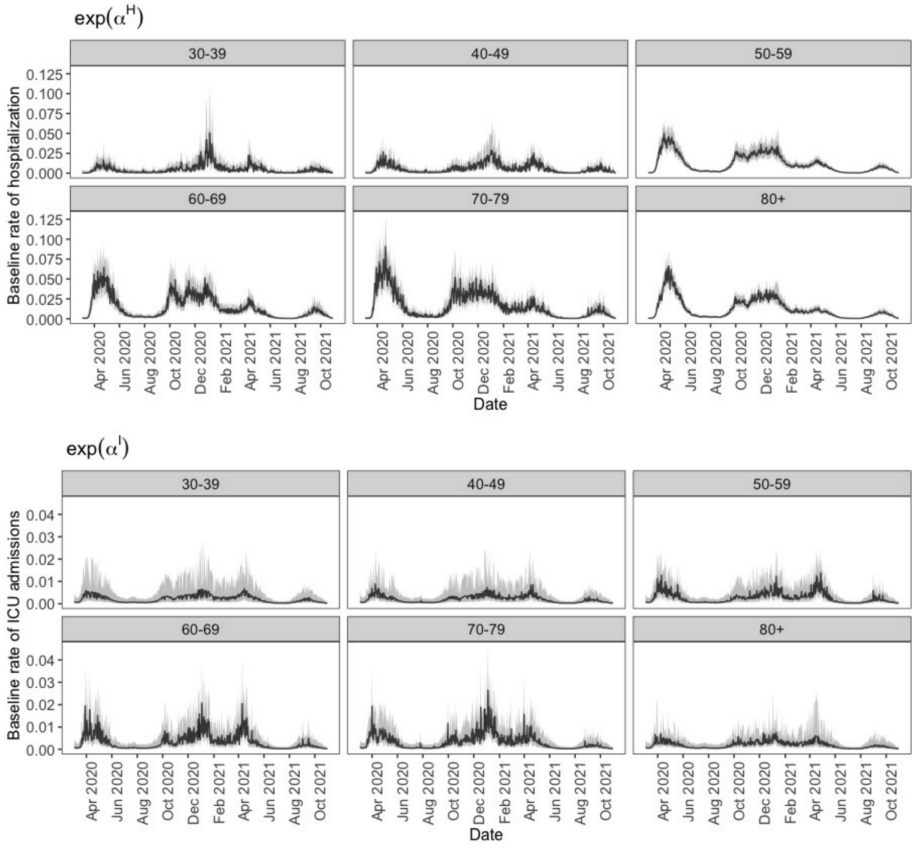

FIGURE 4 | Posterior summaries (mean [solid lines] and limits of 95% posterior credible intervals [shaded area]) for the baseline rates of hospitalizations and ICU admissions for each age group. The top panel shows the baseline rates of hospitalization, and the bottom panel shows the baseline rates of ICU admission.

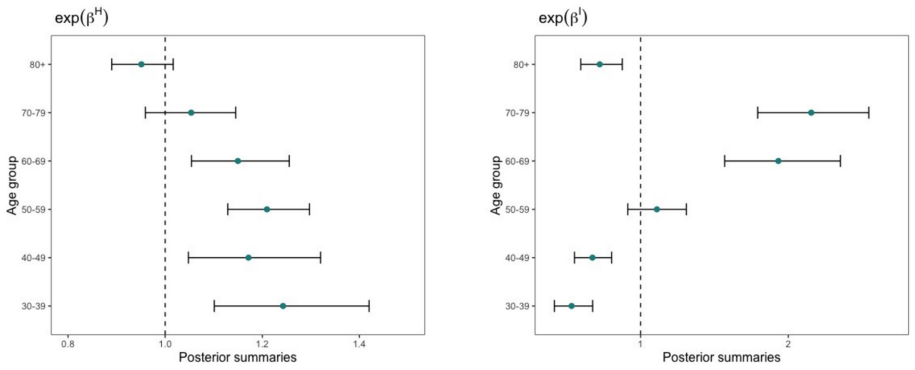

FIGURE 5 | Posterior summaries (mean [solid circles] and limits of 95% posterior credible intervals [line segments]) by age group. The left panel shows the effect of the proportion of male cases on hospitalizations. The right panel shows the effect of the proportion of male hospitalizations on ICU admissions.

the expected number of hospitalizations by 21%. This is in alignment with other studies as male cases tend to be more serious than female cases (Jin et al. 2020). For the 70–79 and 80+ age groups, one falls within the posterior credible interval of the exponential of $\exp(\beta^H)$, which suggests there is no evidence that the proportion of male cases is associated with these hospitalizations.

Focusing on the ICU admissions model (right panel of Figure 5), for individuals below 50, the proportion of hospitalized males decreases the RR of ICU admissions. On the other hand, for individuals between 60 and 79, an increase of one standard deviation of the proportion of hospitalized males almost doubles the rate of ICU admissions. This is in line with the data (Figure S4), as these age groups have a higher number of ICU admissions.

The effect of the proportion of vaccinated people, $\exp(\delta)$, has a posterior mean of 1.02. Still, the 95% credible interval (0.876, 1.18) includes one suggesting that there is no association between vaccination and the log of the risk of hospitalization for

the period considered. A possible explanation is that for most of the observed period, the proportion of vaccinated people was below 1% of the population, and the increase in the number of fully vaccinated people occurred when the fourth wave of the pandemic was still ongoing.

The probability of having no ICU admissions for each day was modelled as a linear function in the logit scale of the number of hospitalizations (Table S3). For age groups below 50, the probabilities do not approach zero indicating that these groups are the least likely to go into the ICU. On the other hand, age groups between 50 and 79 have periods where these probabilities reach zero, indicating that at least one individual is likely to get admitted into the ICU (Figure S5).

4 | Discussion

We proposed a joint model for the daily counts of hospital and ICU admissions due to COVID-19 during the four waves experienced in Quebec, Canada, between March 2020 and October 2021. Our proposed approach takes advantage of the realized correlation between these two time series and imposes a hierarchical structure across the different age groups. Moreover, it allows for a non-linear and persistent effect of the number of cases of COVID-19 on the log rate of hospitalizations. This is done through a transfer function model that naturally accommodates the persistence of the effect of cases over time. As inference is performed following the Bayesian paradigm, uncertainty about the estimates is naturally obtained.

For modelling the ICU admissions, including the hurdle model was crucial to account for the excess of zeros. The idea behind the hurdle model is that a random variable is modelled using two parts: the first which is the probability of attaining value 0, and the second part models the probability of the non-zero values. The interpretation of our model then follows that one process governs if an individual is admitted to the ICU, and another process governs how many ICU admissions occur. The results show that individuals between 50 and 69 are more likely to be admitted to the ICU.

Our analysis confirms the hypothesis that the rate of hospitalization varies with age group. The proposed model was able to capture the differences across age groups in hospitalizations and ICU admissions, while simultaneously accounting for a delayed association between the number of COVID-19 cases and the log risk of hospitalizations via a transfer function. Transfer functions are flexible as they do not require fixing the lag at which the influence of cases on the risk of hospitalization diminishes. Our results suggest that an increase in the number of cases results in a persistent increase in the rate of hospitalizations, especially for the age group 50–59.

As in any data analysis, we need to make certain assumptions to be able to make inference in the face of the limitations of the data. We assume that the date of ICU admission of an individual is the same as the date they were hospitalized because we do not have information on the number of days between hospitalization and ICU admission. Additionally, the analysis is limited to cases registered by hospitals in Quebec. Nevertheless, this analysis provides valuable insights regarding the rates of hospitalization and ICU admission by age group and displays the advantages of using joint temporal models for the study of epidemiological data. One of the possible improvements in the model would be to have vaccination data by age group and for a longer period to show the possible effect of vaccination on the reduction of the number of hospitalizations. Vaccination started with the older age groups for whom the fourth wave of hospitalizations is of lower magnitude. Further research would be required to determine this effect.

While this paper presents a post hoc analysis of the data, the proposed models can be used to monitor the situation in real time during a pandemic, requiring sequential updating of the model. This can be a powerful tool for assisting decision-makers when predicting the number of hospital and ICU beds required on a given day. Additionally, the model can jointly predict the number of patients admitted with a specific disease and the corresponding number of treatments or specialized medical equipment required. It accommodates the current public health situation and provides clear uncertainty quantification of the predictions of interest. Moreover, beyond a hospital setting, the proposed model can be useful in diverse areas such as marketing, for example, the number of loyalty members in a store and the number of purchases made.

Author Contributions

Mariana Carmona-Baez: writing – original draft (lead), writing – review and editing (equal), software (lead), methodology (equal), visualization (lead). **Alexandra M. Schmidt:** conceptualization (lead), supervision (lead), formal analysis (lead), methodology (lead), writing – review and editing (equal). **Shirin Golchi:** methodology (equal), writing – review and editing (equal). **David Buckeridge:** conceptualization (supporting).

Acknowledgements

Carmona-Baez acknowledges the support of the Institut de valorisation des données (IVADO) Fundamental Research Project (PRF-2019-6839748021) and the Quantitative Life Sciences PhD programme. Schmidt was supported by IVADO (Fundamental Research Project, PRF-2019-6839748021) and the Natural Sciences and Engineering Research Council (NSERC) of Canada (Discovery Grant RGPIN-2017-04999). Golchi was supported by a Discovery Grant from the Natural Sciences and Engineering Research Council of Canada (NSERC) and a Chercheurs-boursiers (Junior 1) award from the Fonds de recherche du Québec–Santé (FRQS).

Conflicts of Interest

The authors declare no conflicts of interest.

Data Availability Statement

The data that support the findings of this study are openly available in jointtemporalmodel at https://github.com/mcarmonabaez/jointtemporalmodel.

References

Alves, M. B., D. Gamerman, and M. A. R. Ferreira. (2010). "Transfer Functions in Dynamic Generalized Linear Models." *Statistical Modelling* 10, no. 1: 3–40.

Caramelo, F., N. Ferreira, and B. Oliveiros. (2020). "Estimation of Risk Factors for Covid-19 Mortality-Preliminary Results." *MedRxiv*, 2020.02.24.20027268. https://doi.org/10.1101/2020.02.24.20027268.

Chyon, F. A., M. N. H. Suman, M. R. I. Fahim, and M. S. Ahmmed. (2022). "Time Series Analysis and Predicting Covid-19 Affected Patients by ARIMA Model Using Machine Learning." *Journal of Virological Methods* 301: 114433.

Cohen, J. F., D. A. Korevaar, S. Matczak, M. Chalumeau, S. Allali, and J. Toubiana. (2021). "Covid-19–Related Fatalities and Intensive-Care-Unit Admissions by Age Groups in Europe: A Meta-Analysis." *Frontiers in Medicine* 7: 560685.

Davies, N. G., P. Klepac, Y. Liu, K. Prem, M. Jit, and R. M. Eggo. (2020). "Age-Dependent Effects in the Transmission and Control of Covid-19 Epidemics." *Nature Medicine* 26, no. 8: 1205–1211.

Gelman, A., and D. B. Rubin. (1992). "Inference From Iterative Simulation Using Multiple Sequences." *Statistical Science* 7, no. 4: 457–472.

Jin, J.-M., P. Bai, W. He, et al. (2020). "Gender Differences in Patients with Covid-19: Focus on Severity and Mortality." *Frontiers in Public Health* 8: 545030.

Lipsitch, M., and N. E. Dean. (2020). "Understanding Covid-19 Vaccine Efficacy." *Science* 370, no. 6518: 763–765.

Moghadas, S. M., T. N. Vilches, K. Zhang, et al. (2020). "The Impact of Vaccination on Covid-19 Outbreaks in the United States (preprint)."

Oshinubi, K., A. Amakor, O. J. Peter, M. Rachdi, and J. Demongeot. (2022). "Approach to Covid-19 Time Series Data Using Deep Learning and Spectral Analysis Methods." *Aims Bioengineering* 9, no. 1: 1–21.

Ravines, R. R., A. M. Schmidt, and H. S. Migon. (2006). "Revisiting Distributed Lag Models Through a Bayesian Perspective." *Applied Stochastic Models in Business and Industry* 22, no. 2: 193–210.

Watanabe, S., and M. Opper. (2010). "Asymptotic Equivalence of Bayes Cross Validation and Widely Applicable Information Criterion in Singular Learning Theory." *Journal of Machine Learning Research* 11, no. 116: 3571–3594.

West, M., and J. Harrison. (1997). "The Dynamic Linear Model." In *Bayesian Forecasting and Dynamic Models*, 97–142. Germany: Springer.

Supporting Information

Additional supporting information can be found online in the Supporting Information section.